Shape Adaptive Airfoils for Turbomachinery applications: Simulation and Optimization

Authors:

Tobias Müller*, Martin Lawerenz**

*Research Assistant
**Professor

Correspondence:

Tobias Müller
Institute of Thermal Engineering
Department of Turbomachinery
University of Kassel
Germany

Keywords:

Shape Adaptive Airfoils, Optimization, Response Surface Methodology

ABSTRACT

Smart materials and smart structural concepts in flow control have the potential for significant impact on the design and performance of modern turbocompressors. While the benefits of an airfoil whose geometry is variable were investigated in detail in the area of adaptive wings for airplanes, this is a new field for the application in turbomachines. The main focus is on simulations of novel flow control concepts to allow a structural 'morphing' and thus changing the aerodynamic characteristic of the airfoils. LS-DYNA 970 Implicit is used for the calculations. Additionally, shape optimiziations are performed using LS-OPT in conjunction with a parametric mesh generator.

INTRODUCTION

To control the mass flow (operating point) for constant speed machines and to adapt the inlet flow angle (relative Mach Number) of the first rotor, the compressor inlet is equipped with variable Inlet Guide Vanes (IGV). They are working as a regulating valve by adjusting the stagger angle of each airfoil. Thereby, the IGV produce wakes which have an impact on the performance of the following blade rows. They generate as well unsteady aerodynamic forces in the relative frame of reference. A new approach is to actively adapt the surface geometry of the IGV to adjust the desired flow conditions. The boundary layers of a smooth contoured surface can be better controlled in comparison to the strong acceleration and deceleration of the flow in the leading edge area of restaggered guide vanes. Active flow control using a shape adaptive airfoil for guiding vanes has the potential to avoid separation and modify wake behavior, which leads to higher component efficiency due to reduced losses. The operating range with low profile losses could be extended up to 20° [12].

STRUCTURAL CONCEPTS

The structural concepts should provide a smooth contour having no additional gaps to achieve a chordwise camber variation.

Kinematic chain mechanism

A first concept uses a modified kinematic chain mechanism [8] in order to accomplish large deflections. The airfoil is devided into a predefined number of joined segments. A discrete actuator provides a torsional moment M_t to activate the mechanism. The rotation of the first segment is transferred from segment to segment by the kinematics. The surface of the airfoil is made of an additional layer to enable the large deformations with a smooth contour. Fig. 1 (left) shows as an example an airfoil with 5 segments (without the additional layer).

The structural displacements (scale factor $= 5$) are demonstrated in Fig. 1 (right) for an aerodynamic load corresponding to a Mach number of $Ma_{in} = 0.2$. The triangular load distribution is shown in Fig. 6 (right).

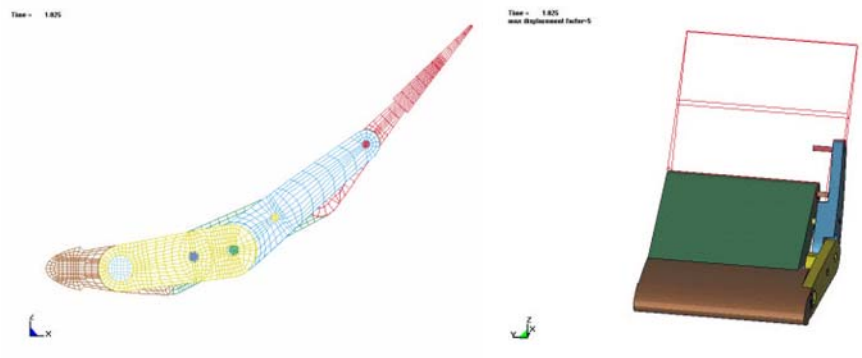

Fig. 1: Kinematic chain mechanism

VOLUME STRETCHING

This concept is based on a hyperelastic material with integrated pressurized channels. Spanwise distributed channels are incorporated into a flexible part of the structure (Fig. 2).

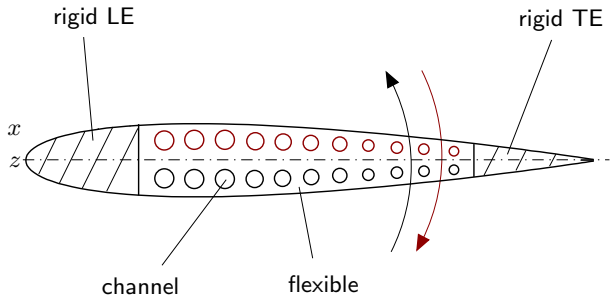

Fig. 2: Adaptive IGV

By means of pressurization of one row of the channels, the trailing edge adaption is activated. The objective is to reach a trailing edge adaption up to $50°$ taking the aerodynamic load into consideration.

Parameter study

3D structural simulations conducted with a NACA0012 geometry are performed to simulate the global structural deformations in this early design stage. A parameter study is carried out to obtain information about relevant design parameters. Therefore, the geometry (Fig. 3) of the integrated channels is varied. The cross section is defined by an ellipse with the semi axes r_1 and r_2. Identical distances between the positions of the channels along the airfoils chord are defined. The values for r_2 are kept constant as 50% of the distance between the camberline and the corresponding surface coordinate of the airfoil. A total number of 30 channels is integrated into the airfoil, whereby 15 are located

close to the suction and pressure surface respectively. The distance from the center of an ellipse to the surface is defined as 30% of the current profile thickness. The rigid leading and trailing edges have a length of 15% of the chord (chord-lenght $= 0.1m$).

Fig. 3: Structural mesh of the airfoil

The Finite Element (FE) calculations are performed by using LS-DYNA [2] Implicit Version 970. The parameter study is conducted using equivalent modulus of elasticity ($E = 5N/mm^2$). The pressurization of the channels is applied by using one pressure p_i for all channels defined by a linear increasing load curve up to $0.5\ MPa$. For the geometry variation no aerodynamic load is applied.

The geometric nonlinear calculation is devided into 20 load steps. The model consists of a very fine mesh with a number of 19940 nodal points and a number of 13128 brick elements to accurately describe the surface deformation. One-point integration solid elements [1] are used to avoid stiffening effects. In this model, a span section of $5\ mm$ is modeled to reduce the computational effort. The symmetry constraint, that a normal to the midsurface (midspan) remains normal to the midsurface after deformation, is applied.

Within a parameter study the ratio of the semi axes

$$s_R = \frac{r_1}{r_2} \tag{1}$$

of the elliptical channels has been varied. Figure 4 summarizes the results.

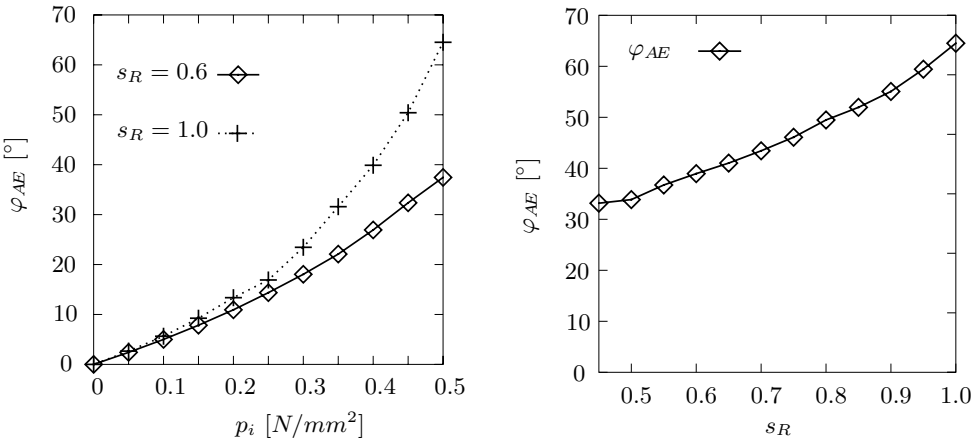

Fig. 4: Deformation as a function of p_i and r_1/r_2

The nonlinear development of the deformation as a function of p_i is shown in Fig. 4 (left). The scaling of r_2 leads to a reduced angle φ_{AE} as depicted in Fig. 4 (right). The

maximum angle φ_{AE} is computed for $s_R = 1.0$. As an example for the deformed airfoil, two meshes are shown in Figure 5.

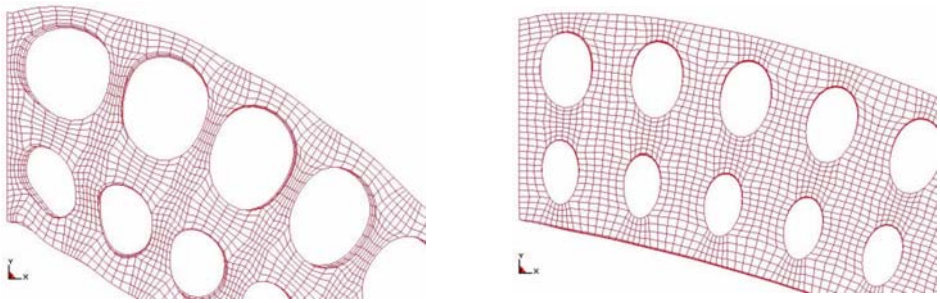

Fig. 5: $s_R = 1.0$ and $s_R = 0.6$ at $p_i = 0.5\ MPa$

Structural behavior under aerodynamic load

A further parameter study is performed at a modified symmetrical airfoil model shown in Fig 6, applying different aerodynamic forces to simulate various flow conditions. One half of the blade is modeled using appropriate symmetrical boundary conditions at midspan. The solid edge of the airfoil is modeled with a thickness of $2\ mm$, whereas the influence of the necessary connections between the channels is neglected. An ellipse geometry with $s_R = 0.6$ is chosen with an actuation pressure of $p_i = 1.0\ MPa$ devided into 20 load steps.

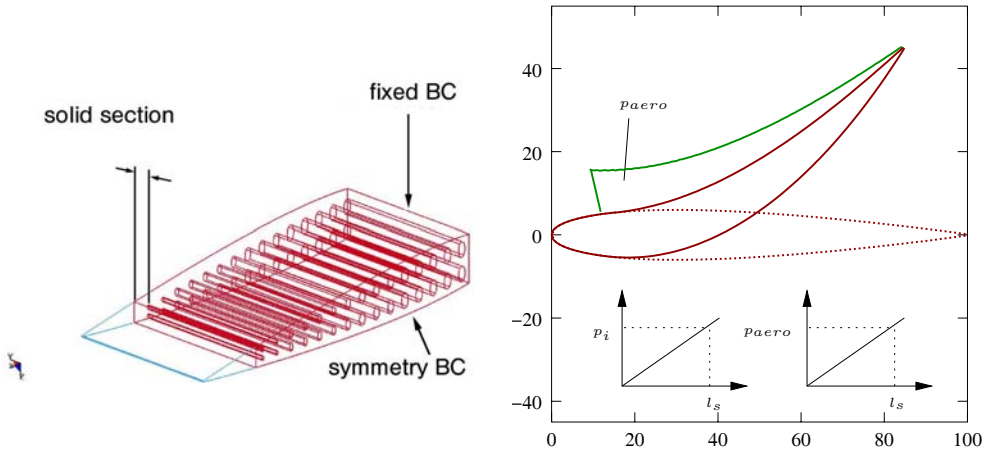

Fig. 6: Boundary Conditions (BC) – pi and p_{aero} as a function of l_s

Static aeroelasticity is assumed during the FE-calculation by the use of an increasing load curve corresponding to the pressurization of the channels. An approximation of the resultant aerodynamic force distribution[1] along the surface of the airfoil is defined as

[1]The aerodynamic force distribution was investigated with aerodynamic computations on S_1-surfaces – conducted using a stream function approach [6].

follows

$$\begin{aligned} p_{aero}(x, \alpha_2) &= p_{PS}(x) - p_{SS}(x) \\ &= p_{a,0}(\alpha_2)\ (1 - \frac{x}{l}) \end{aligned} \tag{2}$$

The results are presented in Fig. 7 (right). Aerodynamic loads up to $F_y = 20N$ are considered for two typical material properties. Together with the given loads, the calculated angles φ_{AE} can be related to an inlet Mach number. A corresponding Mach number of $Ma_{in} = 0.12$ can be calculated for $F_y = 20N$. For the computation with a relative stiff material property ($E = 100\ N/mm^2$), it is easy to see that the influence of the aerodynamic load on the structural response decreases. The disadvantage of such material properties is the required high internal channel pressure p_i which has to be provided. The computed deformation of an airfoil ($p_i = 1.0\ MPa$, $\varphi_{AE} > 50°$, resultant aerodynamic load $F_y = 10N$) is demonstrated in Fig 7 (left).

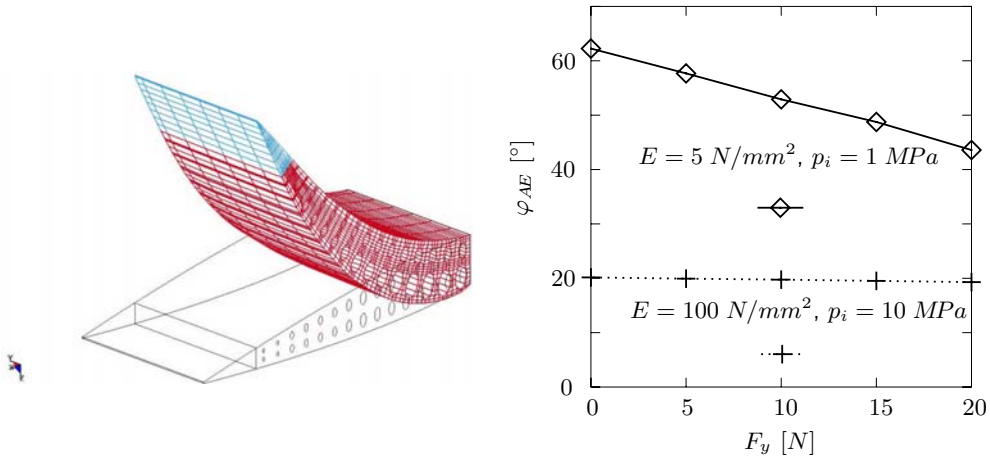

Fig. 7: Computed deformation of the pressurized airfoil – φ_{AE} as a function of F_y

Optimization with LS-OPT

LS-OPT uses approximations (eq. polynomial functions, neural network) of complex system responses to apply mathematical optimization techniques whereby the statistical design of experiments is an important part of constructing high accuracy response models. For further details and a deeper insight into the optimization method implemented in LS-OPT the reader is refered to the open literature on Response Surface Methodology (RSM [9]), the application in structural mechanics [10] and further publications related to LS-OPT [5, 7, 11, 4, 3]. TrueGrid^2, an interactive and batch mesh generator, is used with LS-OPT because of its parameterization capabilities.

The ratios of the ellipse semi axes $s_{R,k}$ of five channels ($k = 1, ..., 5$) are used as design variables $\boldsymbol{x}$. The objective function is constructed using a Least Squares Residual

formulation (LSR).

$$\text{Minimize} \qquad \text{discrepancy (LSR)} \qquad \mathcal{F} = \sqrt{\sum_{j=1}^{m} \left[\frac{dv_j(\boldsymbol{x}, t_j) - Dv_j(t_j)}{\sigma_j(t_j)} \right]^2} \tag{3}$$

where $dv_j(\boldsymbol{x}, t_j)$ represents the y-displacement of a contour node i calculated with LS-DYNA at the load step (implicit)

$$t_j, \qquad j = 1, \ldots, m \tag{4}$$

A target $Dv_j(t_j)$ is specified as the corresponding desired value for each system response. The normalization factor $\sigma_j(t_j)$ is chosen as the same value as the corresponding target value to normalize the objective function value $\mathcal{F}$. A graphical representation of a desired shape adaption is given in Fig. 8.

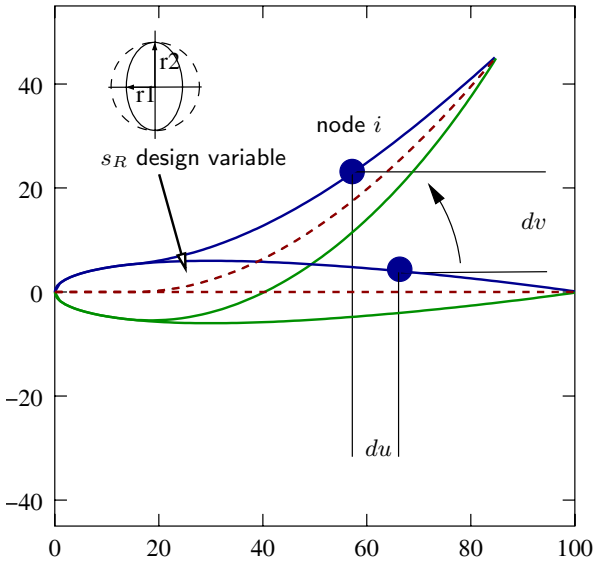

Fig. 8: Desired shape adaption

Hyperelastic material behavior is simulated by use of `MAT_MOONEY-RIVLIN_RUBBER` with the material parameters.

$$c_{10} = 0.3MPa$$
$$c_{01} = 0.49MPa$$

A design variable and objective function value tolerance of $\epsilon_f = \epsilon_x = 0.01$ is chosen as a stopping criterion. The response surface approximation uses 10 experimental points selected from a set of 3^5 experimental base designs (Koshal) with the D-optimal criterion. The response surface approximation is linear. The appropriate result for the history of the objective function value is shown in Figure 9. Table 1 summarizes the optimization results.

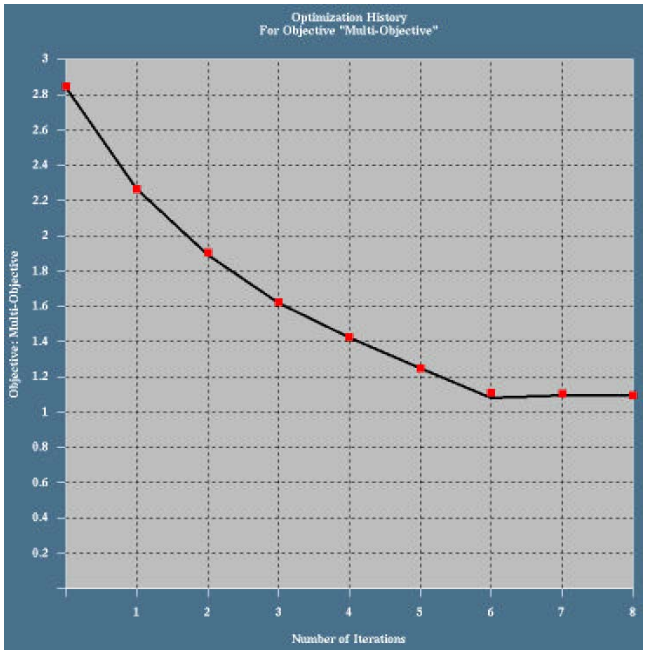

Fig. 9: History: objective function value

Design variable	Lower Bound	Value	Upper Bound
$s_{R,1}$	0.5	0.5	1
$s_{R,2}$	0.5	0.5	1
$s_{R,3}$	0.5	0.7551	1
$s_{R,4}$	0.5	1	1
$s_{R,5}$	0.5	0.8551	1

Table 1: Optimization results

Conclusion

The presented paper describes LS-DYNA simulations and LS-OPT optimizations of geometric variable Inlet Guide Vanes for the application in turbomachines. Adaptive techniques for blade design can reduce losses and avoid separation of the boundary layers on Inlet Guide Vanes. Two structural concepts for the quasi-static shape change of an airfoil are presented. They inlude a kinematic chain mechanism and a concept using a hyperelastic material with integrated pressurized channels (volume stretching). The concept 'volume stretching' has been investigated in detail. Finite element simulations have been conducted to predict the global structural response to geometry and aerodynamic load variation. The results show the strong influence of the geometry of the channel cross section (regarded design variable) on the required internal pressure. Also the magnitude of the aerodynamic load has a strong effect on the achievable deflection. Structural optimizations using LS-OPT lead to a set of design variables to achieve a desired shape change of the airfoil.

Acknowledgement

The authors appreciate the support from Livermore Software Technology Corporation and XYZ Scientific Applications, Inc. for the permission of using LS-DYNA and TrueGrid. Dr. Heiner Müllerschön from DYNAmore for his `*CONTACT`-assistance.

References

[1] Hallquist. *LS-DYNA Theoretical Manual*. Livermore Software Technology Corporation, Livermore, CA, USA, 1998.

[2] Hallquist. *LS-DYNA Keyword User's Manual - Volume 1*. Livermore Software Technology Corporation, Livermore, CA, USA, 2001.

[3] Kok and Stander. Optimization of a sheet metal forming process using successive multipoint approximations. *Structural Optimization, Springer-Verlag*, 18:277–295, 1999.

[4] Stander Kok and Roux. Thermal optimization in transient thermoelasticity using response surface approximations. *International Journal for Numerical Methods in Engineering*, 43:1–21, 1998.

[5] Marzougui Kurtaran, Eskandarin and Bedewi. Crashworthiness design optimization using successive response surface approximations. *Computational Mechanics*, (29):409–421, 2002. Springer-Verlag.

[6] Uelschen M. and Lawerenz M. Design of axial compressor airfoils with artificial neural networks and genetic algorithms. In *Fluids 2000 Conference, June, Denver, AIAA Paper 2000-2546*, 2000.

[7] Stander N. Ls-opt user's manual. *Design Optimization for Engineering Analysis, Version 2*, Livermore Software Technology Corporation, 2002.

[8] Monner H. P., Sachau D., and Breitbach E. Design aspects of the elastic trailing edge for an adaptive wing. pages 14/1–14/8, Ottawa, Canada, October 18–21 1999. Research and Technology Agency.

[9] Raymont and Montgomery. *Response Surface Methodology, Process and Product Optimization using designed experiments*. John Wiley & Sons, New York, Chichester, Brisane, Toronto, Singapore, 1995.

[10] Roux. *Structural Optimization using Response Surface Methodology*. PhD thesis, University of Pretoria, 1997.

[11] Müller T. Comparison of optimization algorithms and their application for identifying material model parameters. *Master of Science thesis, Department of Mechanical Engineering, University of Kassel, Livermore Sofware Technology Corporation*, 2000.

[12] Müller T. and Lawerenz M. Shape adaptive airfoils for turbomachinery applications undergoing large deformations. *AIAA Paper 2003-1561*, pages 1–10, 2003.